0273-2289/96/5903—0259$11.00

Antigen–Antibody Diffusion-Limited Binding Kinetics for Biosensors

A Fractal Analysis

AJIT SADANA* AND ARUNA M. BEELARAM

Chemical Engineering Department,
University of Mississippi, University, MS 38677-9740

Received April 24, 1995; Accepted May 21, 1995

ABSTRACT

A fractal analysis is made for antigen-antibody binding kinetics for different biosensor applications available in the literature. Both types of examples are considered wherein: (1) the antigen is in solution and the antibody is immobilized on the fiberoptic surface, and (2) the antibody is in solution and the antigen is immobilized on the fiberoptic surface. For example, when the antibody is immobilized on the surface, an increase in the antigen *Clostridium botulinum* toxin A concentration in solution leads to (1) a decrease in the fractal dimension value or state of disorder, and (2) a higher rate constant for binding on the fiberoptic surface. An analysis of the effect of the influence of different parameters on the fractal dimension values for a particular example, such as varying treatments or incubation procedures, helps provide insights into the conformational states and reactions occurring on the fiberoptic surface. The analysis of the different examples taken together provides novel physical insights into the state of "disorder" and reactions occurring on the surface. Such types of analysis should help contribute toward manipulating the reactions occurring on the fiberoptic surfaces in desired directions.

Index Entries: Antigen-antibody binding kinetics; biosensors; fractals.

*Author to whom all correspondence and reprint requests should be addressed.

INTRODUCTION

Sensitive detection systems (or sensors) are required to detect a wide range of substances. Sensor applications may be found in the areas of biotechnology, physics, chemistry, medicine, aviation, oceanography, and environmental control. Sensors should be specific, sensitive, stable, easy to use, and inexpensive. Not all of these requirements are satisfied by sensors, and often one compromises. There is an ever-increasing demand not only to utilize sensors in a wide variety of areas, but also to improve the above-mentioned parameters in fields of current utilization. Biosensors are finding increasing application nowadays. The main feature of biosensors is the spatial unity of biomolecules with a signal transducer (*1*). Wise and Wingard (*2*) indicate that biosensors utilize the "cutting edge" principles of biotechnology, electronics, and instrumentation. Scheller et al. (*3*) emphasize the importance of providing a better understanding of the mode of operation of biosensors to improve their sensitivity, stability, and specificity.

The solid-phase immunoassay technique is a convenient means for the separation and/or detection of reactants (for example, antigen) in a solution. The binding of an antigen to an antibody-coated surface (or vice versa) is sensed directly and rapidly. Such a separation and/or detection is possible owing to the high specificity of the analyte for immobilized antibody or antigen, as the case may be. Eddowes (*4*) indicates that optical sensor devices (*5*) that are dependent on the variations in the refractive index are often employed. Harrick (*6*) has suggested utilizing the optical characteristics unique to a reflecting surface between two transparent media. The evanescent wave (that is a part of the internally reflected light beam) allows the optical detection of a reaction occurring at the interface between the two media (*7*). This transduction of a chemical signal to an electrical signal for eventual detection is bound to be complicated. A convenient means is required to "lump" these complexities together effectively.

Furthermore, external diffusion limitations play a role in the analysis of such assays (*4,8–10*). The influence of diffusion in such systems has been analyzed to some extent (*11–16*). Eddowes (*4*) emphasizes that the chemical binding kinetics of the antigen to the immobilized antibody or vice versa, the equilibrium, and the mass transport limitations of the analyte to the surface would constrain the performance of biosensors. It is worthwhile to analyze the diffusion-controlled reactions occurring at the surface, both by conventional as well as by novel techniques, in order that more physical insights may be obtained.

The binding of the antigen to the antibody or vice versa occurs at the interface. Avnir et al. (*17*) have shown that surface irregularities (that are bound to occur as the antigen or the antibody is immobilized to the biosensor surface [optical fiber]) may be characterized using Mandelbrot's

non-Euclidean fractal geometry (*18*). Avnir et al. (*17*) emphasize that for particulate materials, surfaces of progressively higher irregularity are characterized by progressively higher fractal dimensions. Pfeifer and Obert (*19*) emphasize that fractals are disordered systems. This disorder can be described in terms of nonintegral dimensions.

Kopelman (*20*) indicates that surface diffusion-controlled reactions that occur on clusters or islands are expected to exhibit anomalous and fractal-like kinetics. These fractal kinetics exhibit anomalous reaction orders and time-dependent rate (for example, binding) coefficients. The time-dependent adsorption rate coefficients observed experimentally (*21,22*) may also be owing to nonidealities or heterogeneities on the surface. Antibodies are heterogeneous, and their immobilization on a fiber-optic surface, for example, would exhibit some degree of heterogeneity. This is a good example of a "disordered system," and a fractal analysis is appropriate for such systems. In addition, the antigen–antibody reaction on the surface is a good example of a low-dimension reaction system in which the distribution tends to be "less random" (*20*). A fractal analysis would provide novel physical insights into the diffusion-controlled reactions occurring at the surface. Furthermore, Matushihita (*23*) indicates that the irreversible aggregation of small particles occurs in many natural processes, such as polymer science, material science, immunology, and so forth. These aggregation processes frequently result in the formation of complex materials, which can be described by fractals (*24*). Daccord (*25*) emphasizes that when too many parameters are involved in a reaction, the fractal dimension for reactivity may be useful as a "lumped" parameter.

Douglas et al. (*26*) indicate that quite a few physical processes are related to the exterior Dirichlet problem for Laplace's equation (*27*). The capacity determines the steady-state flux of mass, energy, or some other quantity from a solution to arbitrary shaped objects. Douglas et al. (*26*) have proposed a probabilistic method involving hitting the "probed" objects with random walks from an enclosing surface. These authors developed an asympotically exact expression for the temporal reaction rate toward an arbitrarily distributed, arbitrarily shaped collection of "reactive" objects that are embedded in a nonreactive planar surface. A random walk algorithm for calculating the rate by computer simulation has been implemented. In our case, the "probed" object is the antigen or antibody immobilized on the (nonreactive planar surface) biosensor surface. Douglas et al. (*26*) emphasize that these reactive objects are allowed to possess a fractal shape. The analysis of Douglas et al. (*26*) is of a general enough nature, since these authors emphasize that the engineering literature is a rich source of capacitance solution (or steady-state flux) on complicated shape or fractal objects. Thus, their suggested method is applicable to a wide variety of engineering problems.

Stenberg and Nygren (*13*) have emphasized that protein adsorption systems exhibit behavior similar to that of antibody–antigen systems at the

solid–liquid interface. For example, the influence of surface-dependent intrinsic adsorption and desorption rate constants on the amount of protein adsorption has been analyzed (*21,22*). For protein adsorption, Guzman et al. (*28*) initially proposed that the activation energies for adsorption and desorption are dependent on surface coverage. Similarly, Hunter et al. (*29*) suggest that as the surface coverage increases, the activation energies for adsorption and desorption of proteins increase and decrease, respectively. Kondo and Hagashitani (*30*) have recently analyzed the adsorption isotherms of ribonuclease A (RNase A), cytochrome c, lysozyme, α-lactalbumin, and bovine serum albumin on colloidal particles of polystyrene, styrene/2-hydroxyethyl methacrylate, and silica as a function of pH and ionic strength. The authors propose that lateral interactions between the larger protein molecules are stronger because of the thicker adsorption layers at the solid–liquid interfaces. Cuypers et al. (*21*) analyzed the influence of a variable adsorption rate coefficient on protein adsorption. During studies on the adsorption of ferritin from a water solution to a hydrophobic surface, Nygren and Stenberg (*22*) noted that initially the adsorption rate coefficient of the new ferritin molecules increased with time. Nygren and Stenberg (*12*) also noted a decrease in binding rate with time while studying the kinetics of antibody binding to surface-immobilized bovine serum albumin (antigen) by ellipsometry. They indicated that the decrease in binding rate with time is probably owing to saturation through steric hindrance at the surface. Furthermore, Nygren and Stenberg (*22*) indicate that for surface-immobilized antigen, the binding rate is affected by steric interaction between bound antibodies for surface concentrations $>1\ \mu mol/cm^2$.

Havlin (*31*) has analyzed the diffusion of reactants on and toward fractal surfaces. The author indicates that from an experimental point of view, diffusion toward fractal surfaces has been studied more extensively than diffusion on fractal surfaces owing to the number of applications, such as catalytic reactions. However, the author does emphasize that, theoretically, diffusion toward fractal surfaces has been analyzed much less. Some studies are available. For example, Giona (*32*) has recently analyzed first-order reaction-diffusion kinetics in complex fractal media. This author emphasizes that the analysis of the temporal nature of the diffusion-limited reaction on the surface could play an important role in understanding both the reaction kinetics and the reactions at the interface/surface. For a better physical understanding of reactions at interfaces, it is worthwhile using a fractal analysis to examine, as model examples, the behavior of diffusion-limited antigen–antibody binding on biosensor surfaces.

In this article, the fractal dimension values for the kinetics of antibody–antigen binding in the fiberoptic biosensor systems are presented. Wherever sufficient data are available, the influence of a variable, for example, antigen or antibody concentration in solution or on the surface on the fractal dimension value, is presented and analyzed.

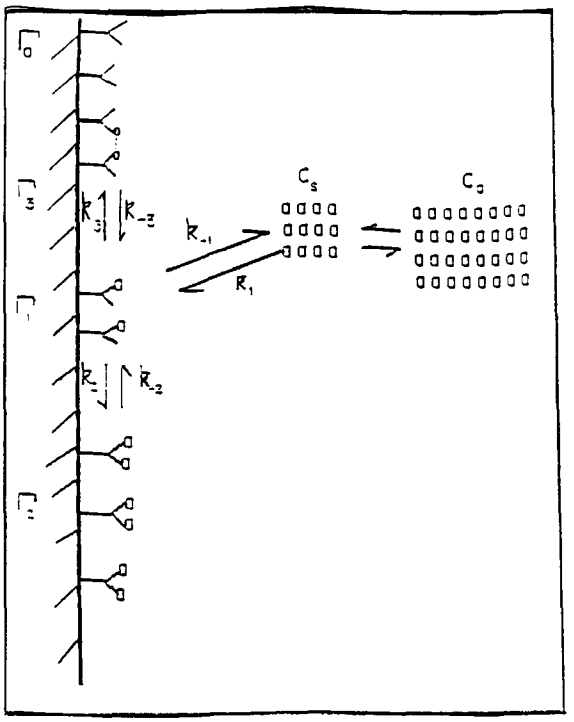

Fig. 1. Elementary steps involved in the binding of the antigen in solution to the antibody covalently attached to the surface (dual-step binding). Involvement of lateral interactions between antibody–antigen complexes on the surface is also shown (k_3, k_{-3}) (*16*).

THEORY

A brief analysis of the binding kinetics of antigen in solution to antibody immobilized on the surface is presented (*15*). The influence of lateral interactions and variable binding coefficients on the surface is also briefly analyzed (*16*). This is followed by a method of estimating actual fractal dimension values for antigen–antibody binding systems utilized in fiberoptic biosensors. Two types of binding systems are analyzed: (1) the antigen is in solution and the antibody is immobilized on the surface, and (2) the antibody is in solution and the antigen is immobilized on the surface.

Antigen in Solution/Antibody on the Surface

Dual-Step Binding

The modeling of binding of an antigen in solution to antibody immobilized on the surface is done by a two-step process. The elementary steps involved in the reaction scheme are shown in Fig. 1 (excluding steps involving k_3 and k_{-3}.

The rate of binding of a single antigen by an antibody is given by (Fig. 1):

$$(d\Gamma_1 / dt) = 2k_1c_s(\Gamma_0 - \Gamma_1 - \Gamma_2) - k_2\Gamma_1c_s + 2k_{-2}\Gamma_2 - k_{-1}\Gamma_1 \quad (1)$$

where Γ_0 is the total concentration of the antibody sites on the surface, Γ_1 is the surface concentration of antibodies that are bound to a single antigen at any time "t," c_s is the concentration of the antigen close to the surface, k_1 and k_2 are the forward reaction rate constants, k_{-1} and k_{-2} are the reverse reaction rate constants. Here, Γ_2 is the surface concentration of the antibody that binds two antigens. The rate at which the antibody binds two antigens is given by:

$$(d\Gamma_2 / dt) = k_2c_s\Gamma_1 - 2k_{-2}\Gamma_2 \quad (2)$$

For initial binding kinetics, after some simplification, Sadana and Sii (*15*) obtained:

$$(d\Gamma_1 / dt) = k_f c_s^2\Gamma_0 \quad (3)$$

The second-order dependence on antigen concentration is not surprising, since two molecules of the antigen can bind to two binding sites on the same antibody molecule.

Diffusion

The diffusion limitation of the reaction scheme can be determined for purely radial diffusion by considering the following equation:

$$(\partial c / \partial t) = (D / r)(\partial / \partial r)[r(\partial c / \partial r)] \quad (4a)$$

where D is the diffusion coefficient.

For a plane surface, Eq. (4a) may be rewritten in dimensionless form as:

$$(\partial y / \partial \Theta) = (\partial^2 y / \partial z^2) \quad (4b)$$

where $y = c/c_0$, $z = x/L$, L is a characteristic length dimension, for example, the diameter of a fiberoptic biosensor, and $\Theta = t/(L^2/D)$. The boundary condition for Eq. (4b) is:

$$(d\Gamma_1 / dt) = D(\partial c / \partial x)|_{x=0} \quad (5a)$$

Here, $x = 0$ represents the origin of the Cartesian coordinate system and is physically the surface of, for example, the fiber to which the antibody is attached. From Eqs. (3) and (5a), one obtains, in dimensionless form:

$$(\partial y / \partial z)|_{z=0} = Dau^2 \quad (5b)$$

where $u = c(0, t)/c_0$, and Da is the Damkohler number and is equal to $k_fL\Gamma_0c_0/D$. The appropriate conditions are:

$$\begin{aligned} c(x, 0) &= c_0 \quad \text{for} \quad x > 0, t = 0 \\ c(0, 0) &= 0 \quad \text{for} \quad x = 0, t = 0 \end{aligned} \quad (5c)$$

Equation (4b) may be solved numerically using the boundary conditions (Eqs. [5b] and [5c]) to obtain solutions for $c(0, t)$ and $\Gamma_1(t)$. The boundary condition is nonlinear, and the solution to Eq. (4b) is obtained by a numerical method (*33*). A similar kinetic analysis for the dual-step binding of antibody in solution to antigen immobilized on the surface is available (*16*).

Influence of Lateral Interactions

Repulsive interactions in the reaction layer have been related to the passivation of surfaces by Cuypers et al. (*21*). The authors state that an initial rapid, often diffusion-limited, rate may be followed by a continuously decreasing adsorption rate. This may arise owing to nonidealities or heterogeneity on the surface, which is shown by Nygren (*34*). Nygren (*34*) determined and analyzed a heterogeneous distribution of adsorbed protein molecules over the surface, indicating that cohesive forces act on the molecules. The attractive interactions would help stabilize the reaction complexes (antibody–antigen) on the surface. Lateral interactions may be treated in two ways: first, by the introduction of a new state and rate constants, and then by a phenomenological model (a power law) for k_1. Γ_3 represents the surface concentration of the antibody–antigen complexes that are involved in lateral interactions on the surface.

The rate of binding of the single arm of the covalently bound antibody to the antigen in solution is given by (Fig. 1) (*16*):

$$\begin{aligned}(d\Gamma_1 / dt) = 2k_1c_s(\Gamma_0 - \Gamma_1 - \Gamma_2 - 2\Gamma_3) \\ - \Gamma_1(k_{-1} + k_2c_s) - k_3\Gamma_1^2 \\ + 2k_{-2}\Gamma_2 + k_{-3}\Gamma_3\end{aligned} \tag{6a}$$

The rate at which the antibody binds two antigens is given by:

$$(d\Gamma_2 / dt) = k_2\Gamma_1c_s - 2k_{-2}\Gamma_2 \tag{6b}$$

The rate at which the antibody-antigen complex molecules laterally interact is given by:

$$(d\Gamma_3 / dt) = k_3\Gamma_1^2 - k_{-3}\Gamma_3 \tag{7}$$

After some simplification, Sadana and Madugula (*16*) obtained:

$$(d\Gamma_1 / dt) = (k_f^2k_3 / k_2^2)\, c_s^2\, [Ab]\, \Gamma_0 \tag{8a}$$

Variable Rate Coefficient

Kopelman (*20*) has recently indicated that classical reaction kinetics is sometimes unsatisfactory when the reactants are spatially constrained on the microscopic level by either wall, phase boundaries, or force fields. Such heterogeneous reactions, for example, bioenzymatic reactions, that occur at interfaces of different phases exhibit fractal orders for elementary

reactions and rate coefficients with temporal memories. In such reactions, the rate coefficient exhibits a form given by:

$$k_1 = k' t^{-b} \qquad 0 \leq b \leq 1 \quad (t \geq 1) \tag{8b}$$

In general, k_1 depends on time, whereas $k' = k_1 (t = 1)$ does not. Kopelman (*20*) indicates that in three dimensions (homogeneous space), $b = 0$. This is in agreement with the results obtained in classical kinetics. Also, with vigorous stirring, the system is made homogeneous, and b again equals zero. However, for diffusion-limited reactions occurring in fractal spaces, $b > 0$; this yields a time-dependent coefficient.

Di Cera (*35*) has analyzed the random fluctuations on a two-state process in ligand binding kinetics. The stochastic approach can be used as a means to explain the variable adsorption rate coefficient. According to Di Cera (*35*), the simplest way to model these fluctuations is to assume that the adsorption rate coefficient $k_1(t)$ is the sum of its deterministic value (invariant) and the fluctuation ($z[t]$). This $z(t)$ is a random function with a zero mean. The decreasing and increasing adsorption rate coefficients can be assumed to exhibit an exponential form (*14,15,21*):

$$k_1 = k_{1,0} \exp(-\beta t) \qquad k_1 = k_{1,0} \exp(\beta t) \tag{8c}$$

Here, β and $k_{1,0}$ are constants.

Sadana and Madugula (*16*) have analyzed the influence of a decreasing and an increasing adsorption rate coefficient on the antigen concentration near the surface when the antibody is immobilized on the surface. The authors noted that for an increasing adsorption rate coefficient, after a brief time interval, as time increases, the concentration of the antigen near the surface decreases, as expected for the cases when lateral interactions are present or absent. Similarly, for a decreasing adsorption rate coefficient, as time increases, the concentration of the antigen near the surface increases continuously for the cases when lateral interactions are present or absent. Furthermore, experimental data presented (*36*) for the binding of HIV virus (antigen) to the antibody anti-HIV immobilized on a surface display a characteristic "disorder." This indicates the possibility of a fractal-like surface. It is obvious that the above biosensor system (wherein either the antigen or the antibody is attached to the surface) along with its different complexities that include heterogeneities on the surface and in solution, diffusion-coupled reaction, time-varying adsorption rate coefficients, and so forth, can be characterized as a fractal system. Examples of biosensors and immunological reactions at interfaces available in the literature are characterized below as fractal systems. Fractal dimension values for these systems are presented and briefly analyzed for different cases, wherein system variables are changed.

Nyikos and Pajkossy (*37*) indicate that a significant amount of work has been done in understanding the role of diffusion and reaction on fractal surfaces (*38–41*). However, the role of diffusion on reaction at fractal

surfaces has not received much attention. These authors did derive a condition to describe nonconventional electrode kinetics during the diffusion-limited transfer of charge across a fractal interface. When the self-similarity property (characteristic of fractal surfaces) was lost, "regular" diffusion was present. It would be of interest to analyze the influence of diffusion on the reactions occurring on fractal surfaces. Does diffusion exacerbate the fractal nature of surfaces, or does it "mask" the fractal nature by "decreasing" its effect on reactions occurring at interfaces? Internal and external diffusion effects have been shown to exacerbate the influence of heterogeneity for other types of systems, for example, enzyme deactivations (*42*).

Havlin (*31*) has briefly analyzed the role of diffusion of reactants toward fractal surfaces. The author indicates that the diffusion of a particle (for example, antibody [Ab]) from a homogeneous solution to a solid surface (the biosensor surface) where it reacts to form a product (antibody–antigen complex) is given by (*37,43–45*):

$$(Ab \cdot Ag) \sim \begin{cases} t^{[(3 - D_f)/2]} = t^p & t < t_c \\ t^{1/2} & t > t_c \end{cases} \quad (9)$$

Equation (9) is a biphasic function of time. Here, D_f is the fractal dimension of the surface. Havlin (*31*) indicates that the crossover value may be determined by $r_c^2 \sim t_c$. Here, p is a coefficient. Above the characteristic length, r_c, the self-similarity of the surface is lost. Above r_c, the surface may be considered homogeneous. For the present analysis, t_c is arbitrarily chosen.

Initially, it was suggested to model the binding curves using Eq. (3) (when no lateral interactions are present) and Eq. (8a) (when lateral interactions are present) (*16*). In these cases, however, the binding rate coefficient is time-invariant. This approach was later modified to include the heterogeneities or degree of inhomogeneity that exists on the biosensor surface. These heterogeneities are better described by a temporal binding rate coefficient that arises out of a fractal analysis (*20*). The fractal analysis is a better description of the real-life situation on the biosensor surface. In addition to the above-mentioned analysis and the fractal analysis, no other explanations have been offered for the seemingly biphasic character exhibited by some of the binding rate curves.

Antigen in Solution/Antibody on the Surface

Anderson and Miller (*46*) have analyzed the binding of the anticonvulsant drug phenytoin using a fiberoptic sensor based on a homogeneous fluorescence energy transfer immunoassay. The reaction chamber used by these authors consists of a small length of cellulose dialysis tubing cemented to the distal end of an optical fiber. The reaction mixture contained phenytoin-valerate-B-phycoerythrin, and Texas red-avidin. Anderson and Miller (*46*) indicate that the biotin and Texas-red avidin system was

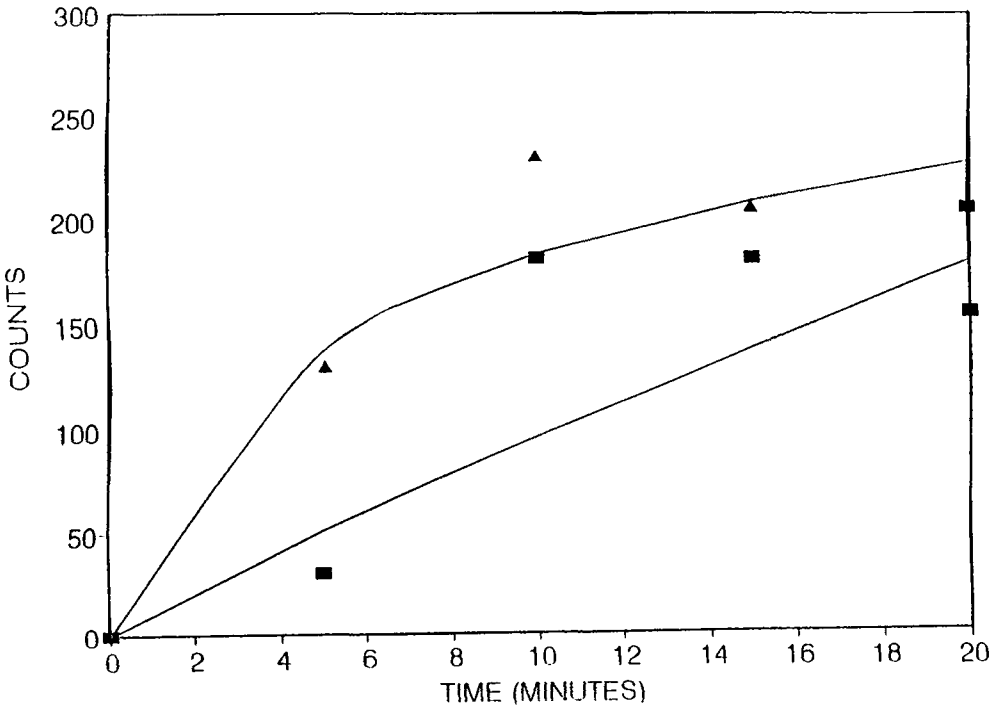

Fig. 2. Theoretical curve using Eq. (9) for the binding of phenytoin in solution to biotin-X-antiphenytoin in BSSG and Texas-avidin immobilized on a fiberoptic biosensor: (■ fresh, (▲) recycled (*46*).

utilized to minimize the denaturation of the antibody on the biosensor surface produced by direct labeling with Texas red. This is of importance to help maintain the stability of the antibody on the fiberoptic surface.

Figure 2 shows the fit of the curve for the binding of 100 μmol/L phenytoin solution to biotin-X-antiphenytoin in BSSG and Texas-red avidin immobilized on a fiberoptic biosensor. Table 1 shows the values of the parameters k, p, and the fractal dimension, D_f, obtained utilizing Eq. (9), a biphasic function of time, to model the experimental data for phenytoin binding. The binding rate coefficient, k, presented in Table 1 was obtained from a regression analysis using Sigmaplot (*51*) to model the experimental data using Eq. (9), wherein $(Ab \cdot Ag) = kt^p$. The k, p, and D_f values presented in Table 1 are within 95% confidence limits. This indicates that the determined parameters are reliable and significant. A fractal dimension value of 1.18 is obtained for this system. No other data are presently available for the system to analyze the influence of different parameters on the fractal dimension value. The few data points available are primarily responsible for the deviation in the value of p obtained. Nevertheless, the fit of the model to the data is reasonably good.

The sensor was transferred from a 100 to 0 μmol/L phenytoin solution and then recycled back to a 100 μmol/l phenytoin solution. Figure 2 shows the binding curve, and Table 1 shows the values of the parameters k, p,

Table 1
Fractal Parameter Values for the Binding of Antigen in Solution to Immobilized Antibody or of Antibody in Solution to Immobilized Antigen

Antigen	Antibody	Surface for immobilization	Detection procedure	k	p	Df	Ref.
Antigen in solution/antibody on surface							
100 μmol/L phenytoin	Biotin-X-antiphenytoin in BBSG and Texas-red avidin	Distal end of an optical fiber	Fluorescence energy transfer	11.69	0.911	1.18	(46)
100 μmol/L phenytoin	Biotin-X-antiphenytoin in BBSG and Texas-red avidin (reused case)	Distal end of an optical fiber	Fluorescence energy transfer	86.6	0.323	2.354	(46)
HIV virus	MAb with a high specificity for prostatic acid phosphatase	5-μm chromium-dioxide magnetic particles of surface area > 40 m^2/g	Competitive binding assay	0.489	0.097	2.806	(47)
HIV virus	MAb with a high specificity for prostatic acid phosphatase	6-mm diameter polystyrene beads	Competitive binding assay	0.067	0.386	2.23	(47)
5 ng/mL of *C. botulinum* toxin A	Affinity-purified antitoxin A	Tapered optical fibers	Sandwich immunoassay using rhodamine-labeled polyclonal anti-toxin A immunoglobulin G	5.37	0.4244	2.15	(48)
25 ng/mL of *C. botulinum* toxin A	Affinity-purified antitoxin A	Tapered optical fibers	Sandwich immunoassay	5.47	0.718	1.564	(48)
50 ng/mL of *C. botulinum* toxin A	Affinity-purified antitoxin A	Tapered optical fibers	Sandwich immunoassay	11.44	0.793	1.414	(48)
100 ng/mL of *C. botulinum* toxin A	Affinity-purified antitoxin A	Tapered optical fibers	Sandwich immunoassay	24.81	0.686	1.628	(48)
200 ng/mL of *C. botulinum* toxin A	Affinity-purified antitoxin A	Tapered optical fibers	Sandwich immunoassay	29.44	0.707	1.586	(48)
0.5 mg/mL anti-IgG-FITC (fluorescein isothiocyanate	Rabbit IgG	Distal sensing tip of a quartz optical fiber	Competitive binding fluorescence immunoassay	50.97	0.355	2.29	(49)

(continued)

Table 1 (Continued)

Antigen	Antibody	Surface for immobilization	Detection procedure	k	p	D_f	Ref.
Antibody in solution/antigen on surface							
Rat thymocytes antigen (Thy-1.1)	0.16 n*M* ^{125}I-labeled F(ab')$_2$ monoclonal bivalent anti-Thy-1.1 antibody	Cell surface	Indirect binding assay with ^{125}I-labeled anti-immunoglobulin	0.031	0.848	1.304	(*50*)
Rat thymocytes antigen (Thy-1.1)	0.16 n*M* ^{125}I-labeled F(ab')$_2$ monoclonal monovalent anti-Thy-1.1 antibody	Cell surface	Indirect binding assay	0.024	0.863	1.274	(*50*)
Rat thymocytes antigen (Thy-1.1)	0.48 ng/μL of ^{125}I-labeled F(ab')$_2$ antibody and 25 μL of 0.5% deoxycholate incubated with 5×10^6 fixed rat thymocytes	Cell surface	Indirect binding assay	26.9	0.114	2.772	(*50*)
Rat thymocytes (Thy-1.1)	0.48 μg/mL of ^{125}I-labeled F(ab')$_2$ was preincubated for 60 min with 0.5 ng/μL of brain Thy-1.1 antigen in 0.5% deoxycholate, then incubated with 5×10^6 fixed rat thymocytes	Cell surface	Indirect binding assay	3.72	0.473	2.054	(*50*)
Rat thymocytes (Thy-1.1)	0.48 μg/mL of ^{125}I-labeled F(ab')$_2$ was incubated with a mixture of 0.5 ng/μL of brain Thy-1.1 antigen in 0.5% deoxycholate, plus 5×10^6 fixed rat thymocytes	Cell surface	Indirect binding assay	32.4	0.0475	2.905	(*50*)
Rat thymocytes (Thy-1.1)	0.72 μg/mL of ^{125}I-labeled rabbit F(ab')$_2$ and 25 μL of 0.5% deoxycholate was incubated with 3×10^6 fixed rat thymocytes	Cell surface	Indirect binding assay	3.766	0.229	2.542	(*50*)
Rat thymocytes (Thy-1.1)	0.72 ng/μL of ^{15}I-labeled rabbit F(ab')$_2$ was incubated with a mixture of 25 μL of thymocyte Thy-1L+antigen (5 ng) in 0.5% deoxycholate plus 3×10^6 rat thymocytes	Cell surface	Indirect binding assay	3.904	0.149	2.702	(*50*)

and the fractal dimension, D_f, obtained by using Eq. (9). It is of interest to note that the D_f value obtained for the recycled case (2.354) is twice the value of D_f obtained (1.178) when the biosensor is used the first time. An increase in the fractal dimension indicates an increase in the "disorder" of the system. Apparently, in this case, the data and the fractal analysis indicate that the recycle and reuse of the biosensor leads to an increasing disorder of the system. The k value for the recycled biosensor (reused) compared to a "fresh" (first-time) biosensor increases by a factor of 7.4 from 11.69 to 86.6. This would indicate that the recycled biosensor is "more sensitive"; however, this is offset to some extent by the higher fractal dimension value for the recycled case.

Ogert et al. (*48*) recently analyzed the detection of *Clostridium botulinum* toxin A using a fiberoptic biosensor. These authors immobilized various affinity-purified antitoxin A antibodies on tapered optical fibers, and performed the assays utilizing different concentrations of the toxin A. Ogert et al. (*48*) utilized a sandwich immunoassay using rhodamine-labeled polyclonal antitoxin A immunoglobin G (IgG). This generated the evanescent fluorescence signal that was analyzed. The assay utilizes the fluorescent complex formed between the botulinum toxin A, an immobilized capture antibody, and a fluorescent antibody. These authors indicate that a fresh fiber was utilized for each study. Also, the following steps were employed: (1) The fiber was placed in the toxin A solution for 10 min, and (2) then, the fiber was placed in the TRITC-antitoxin A IgG solution (5 μL/mL). Figure 3 shows the binding curves, and Table 1 shows the values of the parameters k, p, and D_f obtained by using Eq. (9). The fit of the curves obtained by Eq. (9) is reasonable for the different concentrations of the botulinum toxin A in solution. There seems to be a trend in the values of the fractal dimension obtained with the different toxin A concentrations in solution utilized.

Figure 4 plots the fractal dimension values with the reciprocal of the toxin A concentration in solution. Though there is scatter in the data, the fit of the line of the fractal dimension value, D_f, vs the reciprocal of the toxin A concentration in solution is reasonable. The availability of data points is scarce. More data points would more firmly establish the fit of the line. Nevertheless, the straight line fit indicates that as the concentration of the toxin A in solution increases, the "disorder" on the biosensor surface decreases as noted by a decrease in the fractal dimension value. This indicates that an increase in the toxin A concentration in solution leads to an increasing order of the conformational states of the reaction complex on the fiberoptic biosensor surface. More information for this system and for other systems is required to establish this conclusion more firmly. Nevertheless, this type of information and analysis helps in understanding what is actually happening on the surface. This should then help control the reactions occurring on the surface to advantage.

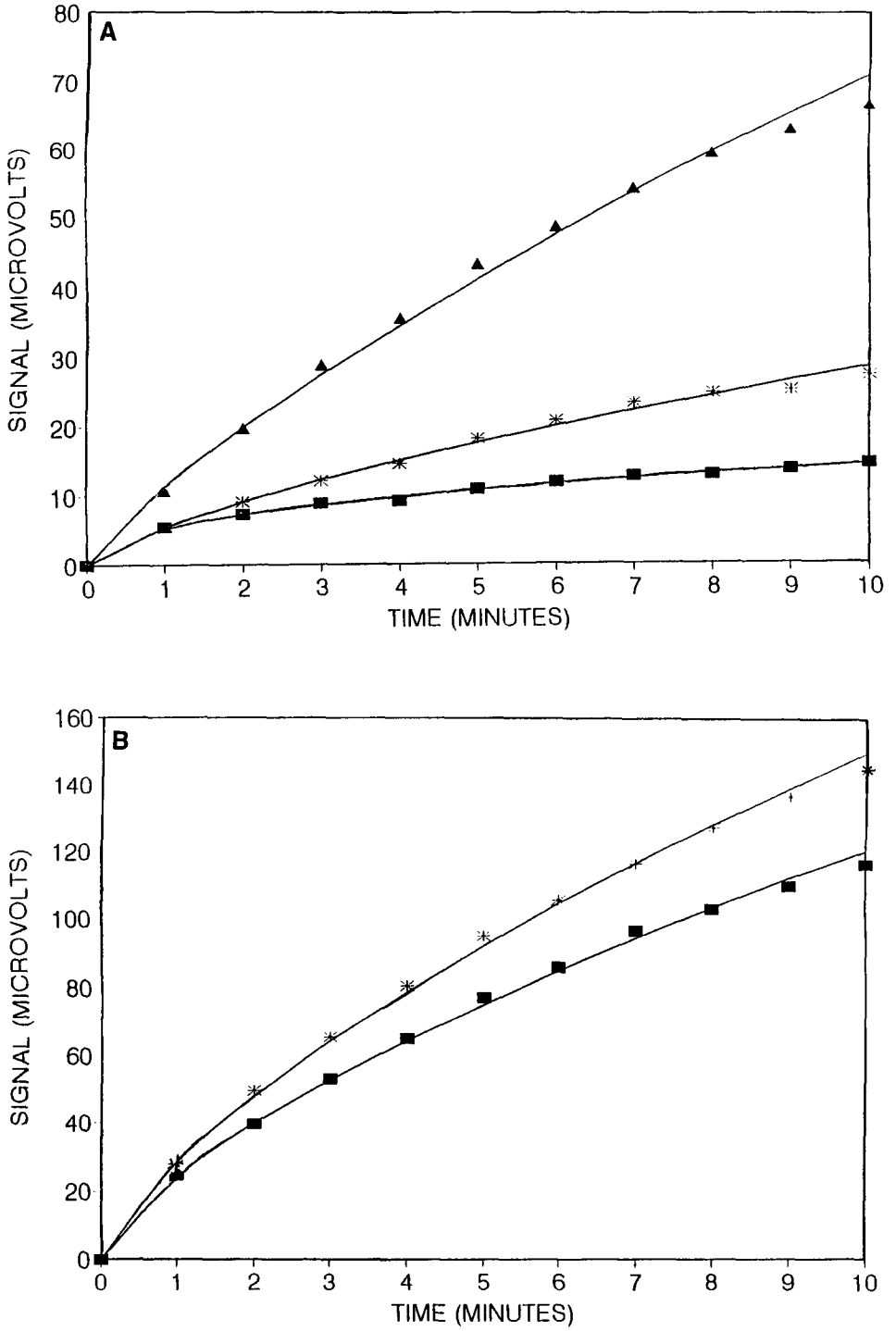

Fig. 3. Theoretical curves using Eq. (9) for the binding of different concentrations of C. *botulinum* toxin A to affinity-purified and antitoxin A antibody immobilized on tapered optical fibers (**A**) (■ 5 ng/mL, (*) 25 ng/mL, (▲) 50 ng/mL, (**B**) (■) 100 ng/mL, (*) 200 ng/mL (*48*).

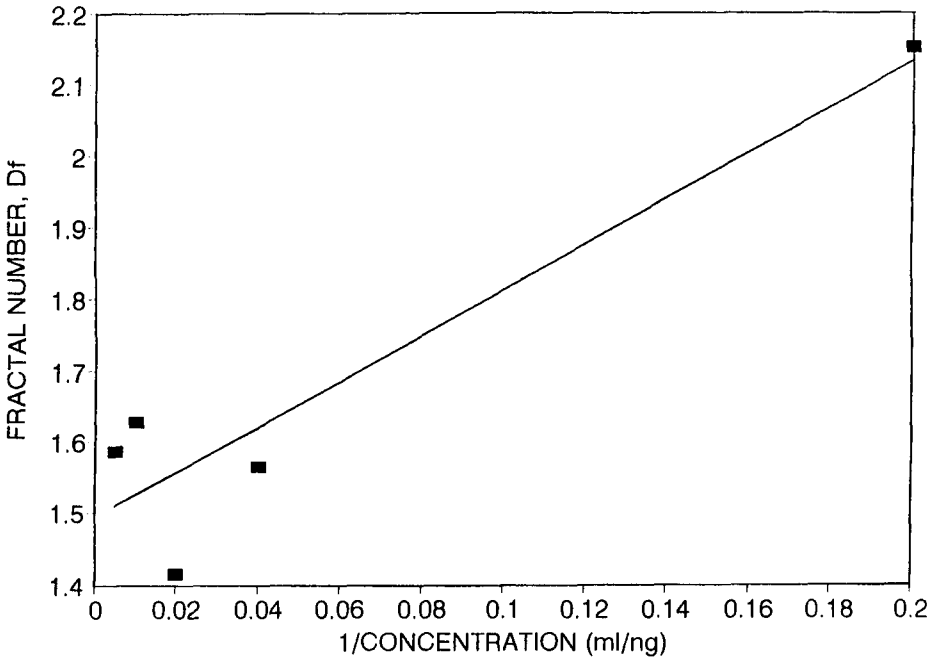

Fig. 4. Increase in the estimated value of the fractal dimension value, D_f, using Eq. (9) with the reciprocal of the *C. botulinum* toxin A concentration in solution.

The next example analyzes the capture of antigens on antibodies immobilized on chromium dioxide particles and on polystyrene beads. Although this is not a fiberoptic biosensor application, it is still worthwhile mentioning, since it involves an immunoassay and assists in decreasing the immunoassay time from typically 4–24 h to 30–45 min. Birkmeyer et al. (*47*) have analyzed the application of novel chromium dioxide magnetic particles to immunoassay development. These authors emphasize that the time frame to complete the assay is largely dependent on the choice of the solid support. These authors have utilized duPont's experience with the manufacture of chromium dioxide for magnetic tape and its biotechnological capabilities with antibodies.

Figure 5 shows the fit of the curve obtained for the binding of HIV virus to the antibody coated on high surface area chromium dioxide particles and on 6-mm diameter polystyrene beads. The coated MAb had a high specificity and affinity for the prostatic acid phosphatase. Birkmeyer et al. (*47*) indicate (and as can be seen from Fig. 5) that 90% of the antigen is bound to the antibody, immobilized on the chromium dioxide particles in the first 3 min. Less than 20% of the antigen is bound to the antibody immobilized on the polystyrene beads in 10 min. These authors emphasize that the total capture by the polystyrene beads is very slow and takes more than 20 h. The fractal dimension values obtained for the binding of the antigen to the antibody on the chromium dioxide particles and on the

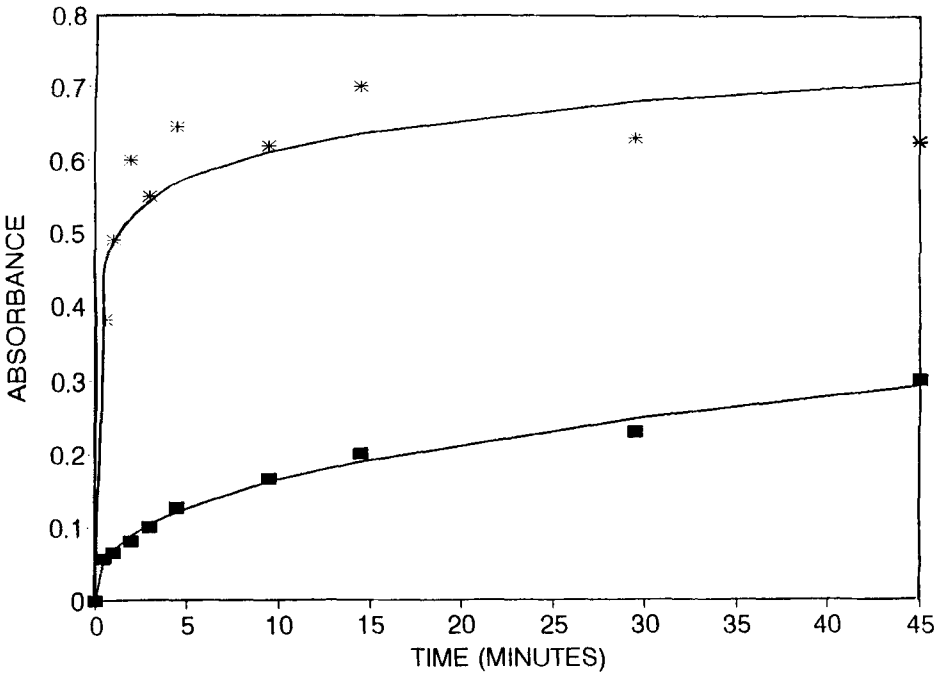

Fig. 5. Theoretical curve using Eq. (9) for the binding of HIV virus in solution to the antibody coated on (*) high-surface area chromium dioxide particles and on (■) 6-mm diameter polystyrene beads (47).

polystyrene beads are 2.806 and 2.228, respectively. The higher fractal dimension value obtained for the chromium dioxide particle compared to the polystyrene bead indicates a higher state of "disorder" for the chromium dioxide particles.

It is of interest to note the k value for the chromium dioxide particles (0.489) is about 72 times higher than the k value for the polystyrene beads. This is the major reason for the reduced assay time for the chromium dioxide particles compared to the polystyrene beads. This is in agreement with the greater surface area of the chromium dioxide particles as compared to the 6-mm diameter polystyrene beads. A greater surface area allows larger amounts of antibody to be immobilized on the particles to help bind and remove the antigen from the solution. The fractal analysis of particulate materials by Avnir et al. (17) indicates that higher surface area particles should, in general, yield higher fractal dimension values. This is consistent with our results.

Furthermore, Birkmeyer et al. (47) emphasize that the special coating applied to the magnetic-tape chromium dioxide particles serves the following purposes:

1. It prevents chromate leaching and improves hydrolytic stability;
2. The coating produces a modified surface that reduces nonspecific binding; and

3. The coating improves the surface for the covalent attachment of the antigens to the antibodies.

This significantly enhances the stability and the yields of the immunoassay. Items (2) and (3) are also of interest in the development of fiberoptic biosensors, and it would be of interest to correlate these modifications to fractal dimension values:

1. To assist in making fiberoptic biosensors more stable;
2. To exhibit higher sensitivities; and
3. To minimize nonspecific binding.

Antibody in Solution/Antigen on the Surface

The theoretical analysis is similar to the one presented above and is available in the literature (*16*). It is not presented here to avoid repetition of what is already available in the literature.

Tromberg et al. (*49*) have recently analyzed the binding of antirabbit IgG in solution to rabbit IgG covalently immobilized on the distal sensing tip of a quartz optical fiber. The authors utilized a competitive binding fluorescence immunoassay. Tromberg et al. (*47*) emphasize that the direct attachment of antibody or antigen via organosilanating reagents is preferred compared to utilizing membrane or gel-entrapped reagent phases. This is because mass transport and immunochemical kinetics severely limit sensor response times. Furthermore, these authors emphasize that once the optical fibers (biosensors) were ready, they were rinsed in phosphate-buffered saline (PBS) and stored in 1% ovalalbumin/PBS at 4°C in order to minimize the effect of nonspecific binding. This permitted the biosensors to be stable for several weeks.

Figure 6 shows the binding of the 0.5 mg/mL stirred anti-IgG-FITC solution to the IgG immobilized on the biosensor (*49*). Table 1 shows the values of the parameters k, p, and the fractal dimension, D_f, obtained utilizing Eq. (9) to help model the experimental data for IgG binding. A fractal dimension value of 2.29 is obtained for this system. No other data are presently available for this system to analyze the influence of different parameters on the fractal dimension value. The few data points available are primarily responsible for the deviation in the value of p obtained. Nevertheless, the fit of the model to the data is reasonably good. The fractal dimension value of 2.29 provides a "composite" number for the "disorder" of this system, wherein diffusion of a reactant to a surface does influence the fractal nature of the surface. It would be of interest to estimate quantitatively the influence of diffusion on the "disordered state" or fractal nature of the surface. Tromberg et al. (*49*) emphasize that signal levels obtained by stirring 1-mL samples for 5 min were about the same as those obtained from 1-mL unstirred samples. This indicates that mass transport limitations are present for high-affinity antibodies, which exhibit rapid antigen-antibody binding kinetics (*12,52*).

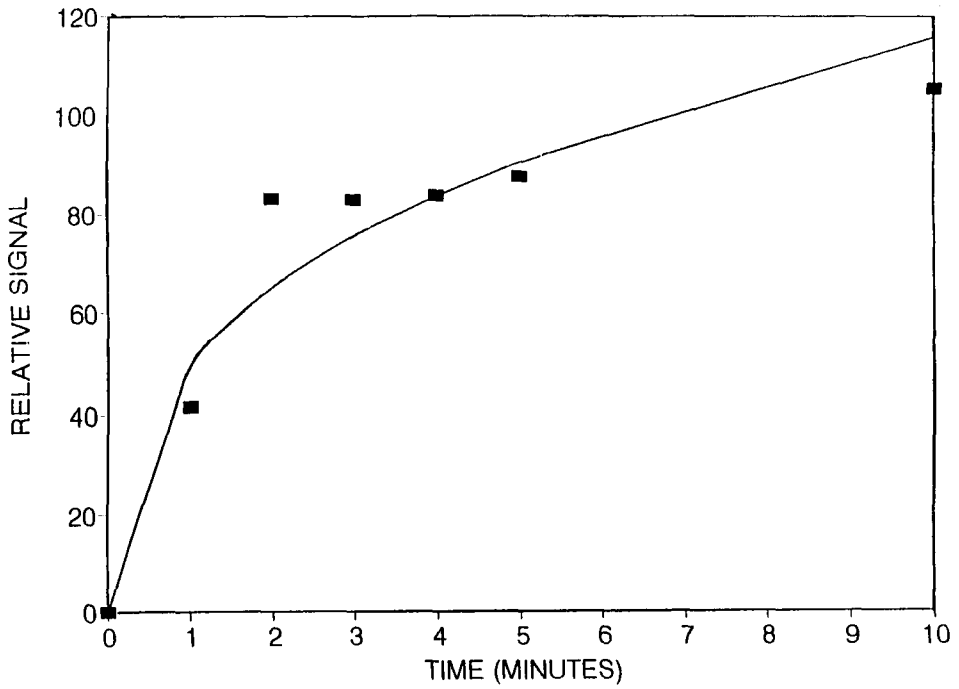

Fig. 6. Theoretical curve using Eq. (9) for the binding of antirabbit IgG in solution to rabbit IgG covalently immobilized on the distal sensing tip of a quartz optical fiber (*49*).

Mason and Williams (*50*) indicate that antibodies are finding increasing utilization for the identification, assay, and purification of membrane molecules. These authors indicate that indirect binding assays with ^{125}I-labeled anti-immunoglobulin can be utilized in several ways. Letarte-Muirhead et al. (*53,54*) and Morris and Williams (*55*) have utilized binding assays to purify Thy-1 antigen (a membrane antigen). Indirect binding assays may also be utilized to analyze other complex antisera (*56–58*). Mason and Williams (*50*) have recently analyzed the kinetics of association and dissociation of antibody interactions with cell-surface antigens in polymeric or monomeric forms. These authors utilized MAbs since conventional antibodies are heterogeneous and are present in low concentrations in serum. Useful results from experiments performed on conventional antibodies are difficult to obtain.

Figure 7A shows the fit of the curve obtained for the binding of 0.16 nM of the ^{125}I-labeled F(ab′)$_2$ bivalent MAb and the ^{125}I-labeled F(ab′) monovalent monoclonal anti-Thy-1.1 antibody to antigen from rat thymocyte (Thy-1.1) on the cell surface. This is clearly not a fiberoptic biosensor application. Nevertheless, an immunological reaction takes place here, and the physical insights gained should be of assistance to understanding immunological reactions on a fiberoptic biosensor surface. Table 1 shows the values of the parameters for k, p, and the fractal dimension, D_f, obtained

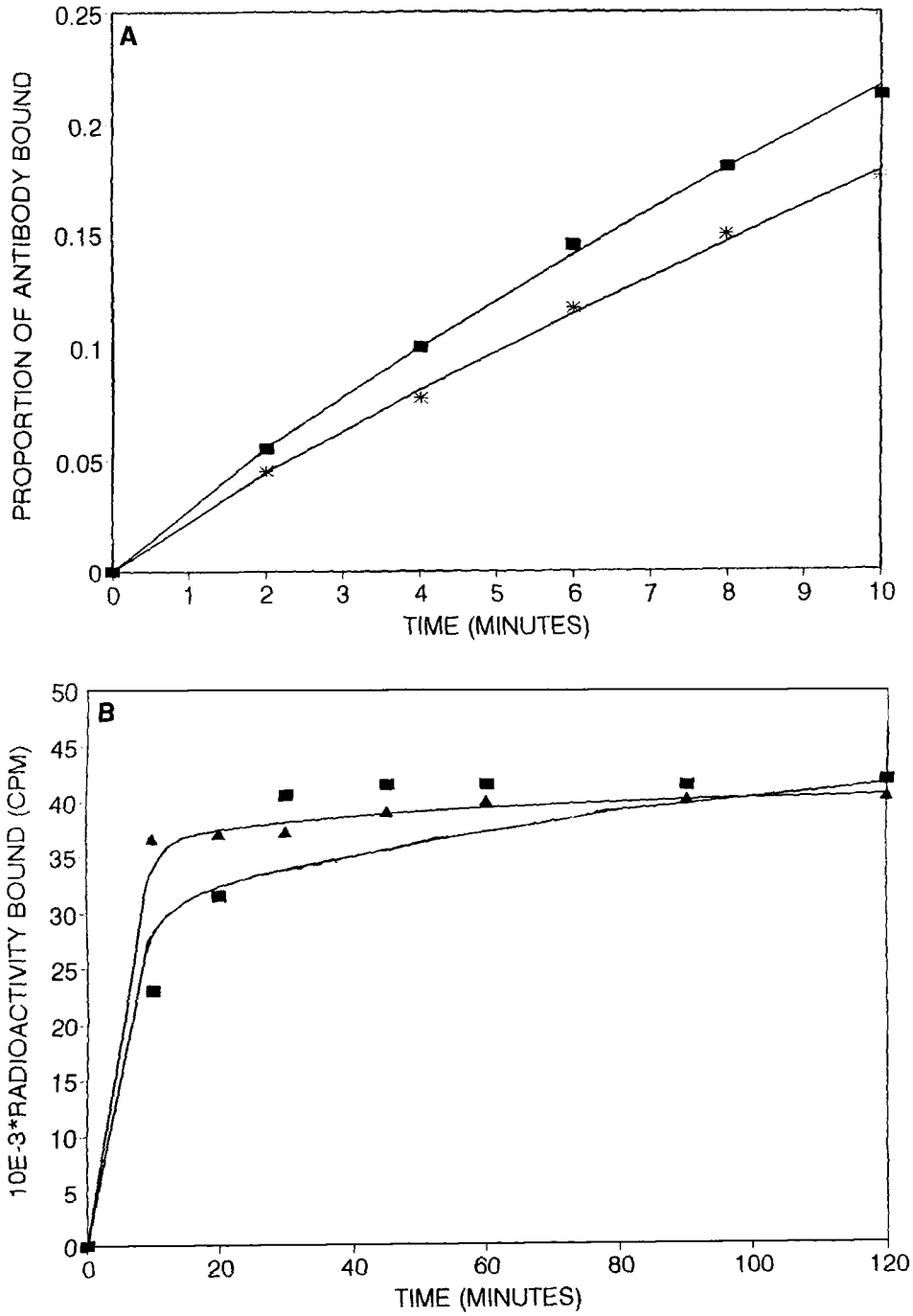

Fig. 7. (**A**) Theoretical curve using Eq. (9) for the binding of ^{125}I-labeled F(ab')$_2$ bivalent MAb (■) and ^{125}I-labeled F(ab') monovalent F(ab') antibody (*) to antigen from rat thymocyte (Thy-1.1) on the cell surface. (**B**) Theoretical curve using Eq. (9) for the binding of ^{125}I-labeled F(ab')$_2$ and 25 μL of 0.5% deoxycholate incubated with 5 × 10^6 fixed rat thymocytes (■) without and (▲) with 25 μL of Thy-1 antigen.

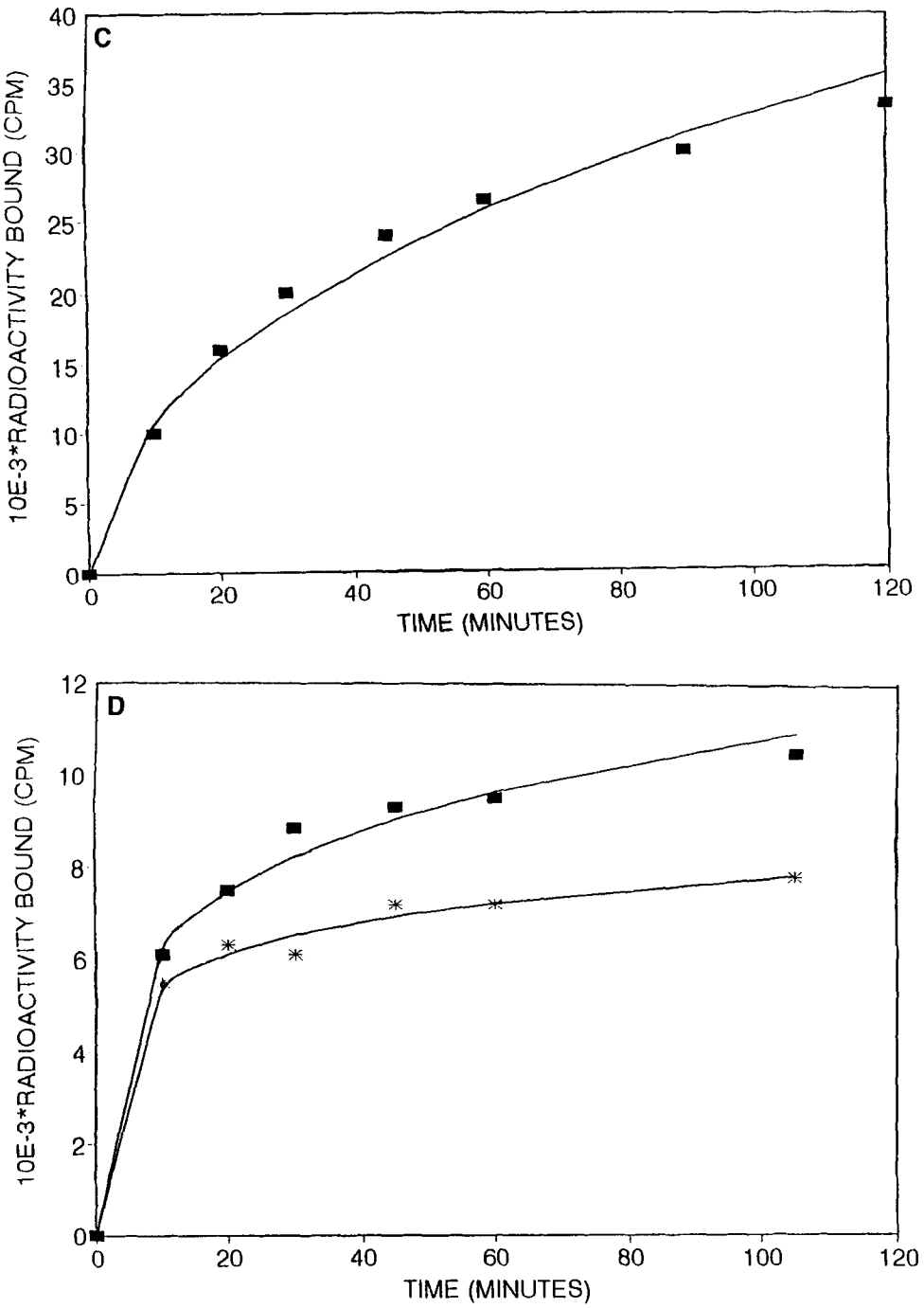

Fig. 7. (*cont'd*). (**C**) Theoretical curve using Eq. (9) for the binding of ^{125}I-labeled F(ab')$_2$ and 25 μL of Thy-1 antigen (12.5 ng) in 0.5% deoxycholate. After 60 min of incubation, 5 × 10^6 fixed rat thymocytes were added to the incubated mixture. (**D**) Theoretical curve using Eq. (9) for the binding of 25 μL of ^{125}I-labeled antibody and 25 μL of 0.5% deoxycholate with 3 × 10^6 fixed rat thymocytes, and (■) without and (*) with Thy-1 + antigen (5 ng) (*50*).

by utilizing Eq. (9) to model the experimental data for $F(ab')_2$ and F(ab') binding. Fractal dimension values of 1.304 and 1.274 are obtained for the bivalent $F(ab')_2$ and the monovalent F(ab') antibody, respectively. The fractal dimension values obtained for the two antibodies are close (within 2.3%) to each other. Thus, apparently for these cases, the single or double valence of the antibody does not significantly affect the state or "disorder" or the fractal dimension of the surface.

Figure 7B shows the fit of the curve obtained for the binding of 25 μL of 0.5% deoxycholate incubated with 5×10^6 fixed rat thymocytes (50 μL in 5% BSA). Table 1 shows the values of the parameters, k, p, and the fractal dimension, D_f. A fractal dimension value of 2.772 was obtained. The addition of 25 μL of the Thy-1 antigen (12.5 ng) to the above mixture prior to incubation yielded a fractal dimension value of 2.905 (*see* Table 1). Apparently, the addition of the 25 μL of Thy-1 antigen to the mixture prior to incubation increases the fractal dimension slightly by about 5%. This is only a slight increase in the state of the disorder of the system compared to the case when the Thy-1 antigen was not included in the incubation mixture.

It is of interest to note that if 25 μL of the $F(ab')_2$ antibody were preincubated with 25 μL of Thy-1 antigen in 0.5% deoxycholate for 60 min and then incubated with 5×10^6 rat thymocytes, the fractal dimension value, D_f (equal to 2.054), is considerably lower (by about 22.4%) compared to the case when all of the above components were incubated together (D_f = 2.9051). Fig. 5C shows the fit of the curve obtained using Eq. (9), and Table 1 shows the parameter values of k, p, and D_f obtained for this case. Apparently, the order of incubation has a significant impact on the state of the disorder of the antibody on the surface. This would indicate that the incubation method leads to a changed conformational state of the $F(ab')_2$ antibody on the cell membrane surface.

CONCLUSIONS

The fractal analysis of the different antigen–antibody reactions occurring on different biosensor surfaces provides a quantitative indication of the state of disorder of the system or the surface. The fractal analysis of both types of systems wherein (1) the antigen is in solution and the antibody is immobilized on the surface, and (2) the antibody is in solution and the antigen is immobilized on the surface indicates the versatility of the analysis, and facilitates comparisons between the two types of systems. Some examples analyzed include just one or two sets of data points. In these types of systems, the influence of different parameters or variables on the fractal dimension (D_f) was not permissible owing to lack of sufficient data. Nevertheless, the single D_f value, or perhaps the D_f value for two unrelated cases for a particular example did provide a numeric value

for D_f. This provides, at least, some indication of the state of disorder on the surface. However, those cases provide valuable physical insights where (1) a significant amount of analyzable data are available, and (2) where the influence of different parameters on the D_f value would be correlated.

For example, consider the D_f value obtained for the "recycled" biosensor compared to the first-time used biosensor (*46*). The analysis indicates an increase in the fractal dimension value with "reuse." This indicates an increasing amount of disorder or conformational states at the biosensor surface on recycle, at least for this system. The analysis of the Mason and Williams data (*50*), which show different fractal dimension values for different incubation procedures, provides valuable insights into beginning to help control the "disorder" or the extent of different conformational states on the surface.

The analysis of the Ogert et al. (*48*) data on *C. botulinum* toxin A is of particular interest, since one can obtain the influence of *C. botulinum* toxin A (antigen) concentration in solution on the D_f value. The fractal analysis of the Ogert et al. (*48*) data indicates that as the concentration of the *C. botulinum* toxin A in solution increases, the fractal dimension decreases. In fact, the data analysis indicates that the fractal dimension value varies inversely with the *C. botulinum* toxin A in solution. Apparently, in this case, higher concentrations of the antigen in solution minimize the degree of disorder on the biosensor surface (lower D_f values). Thus, one can apparently control the extent of conformational states for *botulinum* toxin A on the surface, at least for this application. More data of this type for this and other antigen–antibody systems are required to help further validate and or modify the above for biosensor applications.

The fractal analysis of different antigen–antibody binding kinetics for different biosensor applications helps provide novel physical insights into the conformational states of the antigen–antibody binding complex on the biosensor surface. The fractal dimension provides a qualitative description of the state of disorder or heterogeneity or degree of inhomogeneity of the antibody–antigen complex on the surface. One may relate the fractal dimension to the experimental parameters. Thus, one has a means by which to control the inhomogeneity on the surface. This assists in the design of biosensors. Also, the fractal analysis helps better describe the kinetics. These types of analyses taken together help begin to form a framework, wherein the data of different researchers working on different biosensors may be compared. The buildup of a data base on conformational states should also assist in improving the sensitivity, stability, and reaction time of biosensors. It may be recommended that further similar studies (theoretical as well as experimental) be carried out to delineate further the conformational states of the antigen–antibody complex on the biosensor surface.

REFERENCES

1. Lowe, C. R. (1985), *Biosensors* **1,** 3–16.
2. Wise, D. L. and Wingard, L. B., Jr. (1991), in *Biosensors with Fiberoptics,* Wise, D. L. and Wingard, L. B., Jr. eds., Humana, Totowa, NJ, pp. vii–viii.
3. Scheller, F. W., Hintsche, R., Pfeifer, D., Schubert, D., Reiedl, K., and Kindervater, R. (1991), *Sensors and Actuators* **4,** 197–206.
4. Eddowes, E. (1987/1988), *Biosensors* **3,** 1–15.
5. Place, J. F., Sutherland, R. M., and Dahne, C. (1985), *Biosensors* **1,** 321–353.
6. Harrick, N. J. (1967), *Internal Reflection Spectroscopy,* Wiley Interscience, New York.
7. Sutherland, R. M., Dahne, C., Place, J. F., and Ringrose, A. S. (1984), *Clin. Chem.* **30/9,** 1533–1538.
8. Giaver, I. (1976), *J. Immunol.* **116,** 766–771.
9. Bluestein, B. I., Craig, M., Slovacek, R., Stundtner, L., Uricouli, C., Walziak, I., and Luderer, A. (1991), in *Biosensors with Fiberoptics,* Wise, D. and Wingard, L. B., Jr., eds., Humana, Totowa, NJ, pp. 181–223.
10. Place, J. F., Sutherland, R. M., Riley, A., and Mangan, C. (1991), in *Biosensors with Fiberoptics,* Wise, D. L. and Wingard, L. B., Jr., eds., Humana, Totowa, NJ, pp. 253–291.
11. Stenberg, M., Stiblet L., and Nygren, H. A. (1986), *J. Theor. Biol.* **120,** 129–142.
12. Nygren, H. and Stenberg, M. (1985), *J. Colloid Interf. Sci.* **107,** 560–566.
13. Stenberg, M. and Nygren, H. A. (1982), *Anal. Biochem.* **127,** 183–192.
14. Sadana, A. and Sii, D. (1992), *J. Colloid Interf. Sci.* **151,** 166–177.
15. Sadana, A. and Sii, D. (1992), *Biosens. Bioelectron.* **7,** 559–568.
16. Sadana, A. and Madugula, A. (1993), *Biotechnol. Prog.* **9,** 259–266.
17. Avnir, D., Farin, D., and Pfeifer, P. (1985), *J. Colloid Interf. Sci.* **103,** 112–123.
18. Mandelbrot, B. B. (1982), *The Fractal Geometry of Nature.* Freeman, San Francisco.
19. Pfeifer, P. and Obert, M. (1989), in *The Fractal Approach to Heterogeneous Chemistry: Surfaces, Colloids, Polymers,* Avnir, D., ed., Wiley, New York, pp. 11–43.
20. Kopelman, R. (1988), *Science* **241,** 1620–1626.
21. Cuypers, P. A., Willems, G. M., Kop, J. M., Jansen, M. P., and Hermens, W. T. (1987), in *Proteins at Interfaces. Physiochemical and Biochemical Studies,* Brash, J. L. and Horbett, T. A., eds., American Chemical Society, Washington, DC, pp. 208–221.
22. Nygren, H. and Stenberg, M. (1990), *Biophys. Chem.* **38,** 67–75.
23. Matushihita, M. (1989), in *The Fractal Approach to Heterogeneous Chemistry: Surfaces, Colloids, Polymers,* Avnir, D., ed., Wiley, New York, pp. 161–179.
24. Mandelbrot, B. B. (1989), in *The Fractal Approach to Heterogeneous Chemistry: Surfaces, Colloids, Polymers,* Avnir, D., ed., Wiley, New York, pp. 3–9.
25. Daccord, G. (1989), in *The Fractal Approach to Heterogeneous Chemistry. Surfaces, Colloids, Polymers,* Avnir, D., ed., Wiley, New York, pp. 187–197.
26. Douglas, J. F., Zhou, H. X., and Hubbard, J. B. (1994), *Phys. Rev. E.* **49,** 5319–5331.
27. Polya, G. and Szego, G. (1951), *Isoperimetric Inequalities in Mathemathical Physics,* Annals of Mathematical Studies, Princeton University Press, Princeton, NJ.
28. Guzmann, R. Z., Carbonell, R. G., and Kilpatrick, P. K. (1986), *J. Colloid Interf. Sci.* **114,** 536–547.
29. Hunter, J. R., Kilpatrick, P. K., and Carbonell, R. G. (1990), *J. Colloid Interf. Sci.* **150,** 344–351.
30. Kondo, A. and Hagashitani, K. (1992), *J. Colloid Interf. Sci.* **150,** 344–353.
31. Havlin, S. (1989), in *The Fractal Approach to Heterogeneous Chemistry: Surfaces, Colloids, Polymers,* Avnir, D., ed., Wiley, New York, pp. 251–269.
32. Giona, M. (1992), *Chem. Eng. Sci.* **47,** 1503–1515.